

Tim Gudmand-Høyer

Note on the moment capacity in a Bubble deck joint

Rapport
BYG· DTU R-074
2003

ISSN 1601-2917
ISBN 87-7877-137-4

Note on the moment capacity in a Bubble deck joint

Tim Gudmand-Høyer

Preface

This note has been made during my Ph.D. study at the Department of Structural Engineering and Materials, Technical University of Denmark (BYG•DTU), under the supervision of Professor, dr. techn. M. P. Nielsen.

I would like to thank my supervisor for valuable advise, for the inspiration and the many and rewarding discussions and criticism to this work.

Thanks are also due to M. Sc. Ph.D.-student Karsten Findsen, BYG•DTU and M. Sc. Ph.D.-student Lars Z. Hansen, BYG•DTU for their comments to the present note.

Lyngby, Oktober 2003

Tim Gudmand-Høyer

Summary

This note treats the subject of anchoring reinforcement bars in slabs where one part of the slab has been cast prior to the other one, whereby a weak construction joint is introduced.

The investigation is based on the theory of plasticity using upper bound solutions to calculate the load carrying capacity.

The note consists of three main sections.

The background theory is treated in section 1 where the basic failure mechanisms are described.

Section 2 describes some special failure mechanisms that might occur in the joint connection.

Sections 3 and 4 illustrate the method through case studies.

Final conclusions are made in section 5.

The investigation is purely theoretical.

Resume

Denne note omhandler emnet beregning af forankringsstyrken af armering i en plade der består af et filigran element og en insitu støbt pladedel. I en sådan plade vil der være et støbeskel og dette støbeskel vil have indflydelse på forankringen af stødarmeringen.

Noten er opdelt i 3 hovedafsnit.

I afsnit 1 opsummeres de grundlæggende brudmekanismer der anvendes i denne note.

I afsnit 2 er der en beskrivelse af de brudmekanismer der vil være aktuelle i forbindelse med et forankringsbrud i en samling.

I afsnittene 3 og 4 illustreres beregningernes anvendelse ved eksempler. Konklusioner findes i afsnit 5.

Denne note indeholder udelukkende teoretiske overvejelser.

Table of contents

1	Background theory	13
2	Failure mechanisms in a joint	17
3	A case study of an actual load carrying capacity	23
4	A case study for a design situation.....	29
5	Literature	36

Notation

The most commonly used symbols are listed below. Exceptions from the list may occur, but this will be noted in the text in connection with introduction of the notation in question.

Geometry

h	Height of a cross-section
b	Width of a cross-section
A_s	Area of reinforcement
δ	Maximum separation width
d	Diameter of the reinforcement
l	Anchorage length
L_s	Length from the joint to the transverse reinforcement, see Figure 2.3.

Physics

f_c	Compressive strength of concrete
f_{ck}	Characteristic compressive strength of concrete
f_{cd}	Design compressive strength of concrete
f_y	Yield strength of reinforcement
f_{yk}	Characteristic yield strength of reinforcement
f_{yd}	Design yield strength of reinforcement
f_{scr}	Stress in the reinforcement at failure
ρ	Reinforcement ratio
Φ	Degree of reinforcement
m_p	Yield moment in pure bending per unit length
ν	Effectiveness factor for concrete in compression
ν_t	Effectiveness factor for concrete in tension
W_i, W_e	Internal and external work, respectively
γ_c	Safety factor, concrete
γ_s	Safety factor, steel

Introduction

In Bubble deck¹ construction there are necessarily joints of different kinds. The in-situ part of the Bubble deck is cast on a prefabricated slab (a filigran deck). In this note the bond strength of the reinforcement is calculated in a joint between two precast slabs. The bond strength is influenced by the casting joint between the precast slab and the in-situ concrete.

¹ Bubble deck is invented by the Danish engineer Jørgen Breuning

1 Background theory

The theory used in this note is the theory of plasticity with some modifications. The theory is described in [1].

For slabs consisting of two parts some special failure mechanisms may occur. The standard failure mechanisms are shown in Figure 1.1. The special failure mechanisms are introduced below.

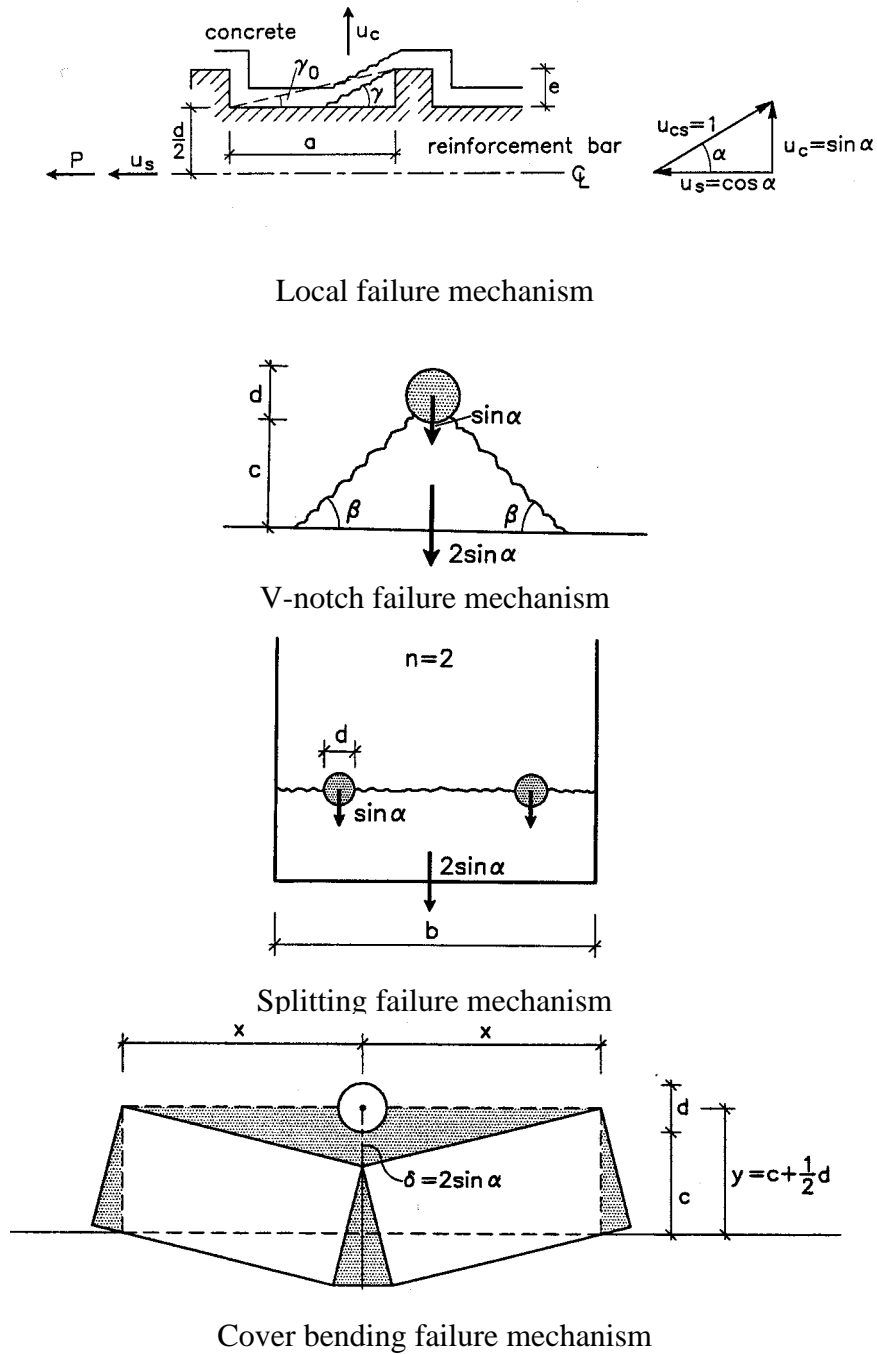


Figure 1.1 Failure mechanisms, [1].

For a failure involving a reinforcement bar subjected to a force P in the direction of the bar, the external work becomes:

$$W_e = P \cos(\alpha) \quad (1.1)$$

The dissipation is calculated as a contribution from a local failure mechanism L , a failure in the surrounding concrete S and a contribution from the reinforcement B . The work equation becomes:

$$nP \cos(\alpha) = nL + S + B \quad (1.2)$$

The average shear stress, the bond strength, becomes:

$$\frac{P}{\pi d l f_{cd}} = \frac{\tau}{f_{cd}} = \frac{\tau_0}{f_{cd}} + \frac{\tau_s}{f_{cd}} + \frac{\tau_B}{f_{cd}}$$

where

$$\frac{\tau_0}{f_{cd}} = \frac{L}{\pi d n l f_{cd} \cos(\alpha)} \quad (1.3)$$

$$\frac{\tau_s}{f_{cd}} = \frac{S}{\pi d n l f_{cd} \cos(\alpha)}$$

$$\frac{\tau_B}{f_{cd}} = \frac{B}{\pi d n l f_{cd} \cos(\alpha)}$$

The bond strength contribution from the local failure of one bar may be calculated as:

For $\alpha - \varphi \geq \gamma_0$

$$\frac{\tau_0}{f_{cd}} = \frac{\nu}{2} \frac{d+e}{d} \frac{e}{a} \frac{1 - \sin(\varphi)}{\sin(\alpha - \varphi) \cos(\alpha)}$$

For $0 \leq \alpha - \varphi \leq \gamma_0$

$$\frac{\tau_0}{f_{cd}} = \frac{\nu}{2} \frac{d+2e-a \tan(\alpha - \varphi)}{d} \frac{1 - \sin(\varphi)}{\cos(\alpha - \varphi) \cos(\alpha)} \quad (1.4)$$

The dissipation in the surrounding concrete depends on the failure mechanism.

If the failure is a V-notch failure the bond strength contribution becomes:

$$\frac{\tau_s}{f_{cd}} = \frac{4}{\pi} \left(\frac{\frac{c}{d} + \frac{1}{2}}{\sin(\beta)} - \frac{1}{2} \right) \left(\frac{1}{2} (1 - \cos(\beta)) + \frac{\rho}{\nu} \frac{\cos(\beta) - \sin(\varphi)}{1 - \sin(\varphi)} \right) \tan(\alpha)$$

where

$$\beta \leq \frac{\pi}{2} - \varphi \quad (1.5)$$

If the failure is a cover bending failure the bond strength contribution for one bar becomes:

$$\frac{\tau_s}{f_{cd}} = \frac{2}{\pi} \left(2 \left(\frac{c}{d} + \frac{1}{2} \right) \sqrt{1 + \frac{\nu}{\rho}} - 1 \right) \rho \tan(\alpha) \quad (1.6)$$

If the failure is a splitting failure the bond strength contribution for one bar becomes:

$$\frac{\tau_s}{f_{cd}} = \frac{2}{\pi} \left(\frac{b}{nd} - 1 \right) \frac{\rho}{\nu} \tan(\alpha) \quad (1.7)$$

The bond strength contribution from transverse reinforcement is:

$$\frac{\tau_B}{f_{cd}} = \frac{f_{scr} \sum A_{sw} u_B}{\pi d n l f_{cd} \cos(\alpha)} \quad (1.8)$$

Note on the moment capacity in a Bubble deck joint

where u_B is the displacement in the direction of the bar, A_{sw} is the area of reinforcement in the failure surface and n the number of bars sharing the reinforcement contribution.

In the expressions above the effectiveness factor ν and the stress in the transverse reinforcement may be calculated as:

$$\begin{aligned}\nu &= \frac{1.8}{\sqrt{f_c}} \leq 1 \quad (f_c \text{ in MPa}) \\ \nu_t &= 1.9 \sqrt{\frac{d}{l}} \leq 1 \\ \rho &= \frac{\nu_t f_t}{f_c} \\ f_{scr} &= 40 \text{ MPa}\end{aligned} \tag{1.9}$$

In the case of bending failure, the moment capacity may be calculated as:

$$m_p = \begin{cases} \left(1 - \frac{1}{2} \frac{\Phi}{\nu}\right) \Phi d^2 f_{cd} & \text{for } \Phi \leq \nu \\ \frac{\nu}{2} d^2 f_{cd} & \text{for } \Phi \geq \nu \end{cases}$$

where

$$\Phi = \frac{A_s f_{yd}}{d f_{cd}}$$

$$\nu = 0.85 - \frac{f_c}{300} \quad \begin{matrix} \text{for } f_y \leq 600 \text{ MPa} \\ \text{for } f_c \leq 60 \text{ MPa} \end{matrix} \tag{1.10}$$

The shear capacity of a rough joint may in general be calculated as:

$$\tau = c' + 0.75 (r f_{yd} + \sigma)$$

where

$$\frac{c'}{f_c} = \frac{0.83}{\sqrt{f_c}} \quad (f_c \text{ in MPa}) \tag{1.11}$$

When the external force gives rise to tensile stresses in the joint the shear capacity should be calculated as:

$$\tau = 0.75 r f_{yd} \tag{1.12}$$

2 Failure mechanisms in a joint

Consider the slab in Figure 2.1 where the bottom consists of two precast slab parts. We now wish to determine the moment capacity in this joint. The moment capacity depends on the possible stress in the reinforcement. It is evident that the tension in the reinforcement in the precast parts has to be transferred through the joint reinforcement and this leads to some special failure mechanisms.

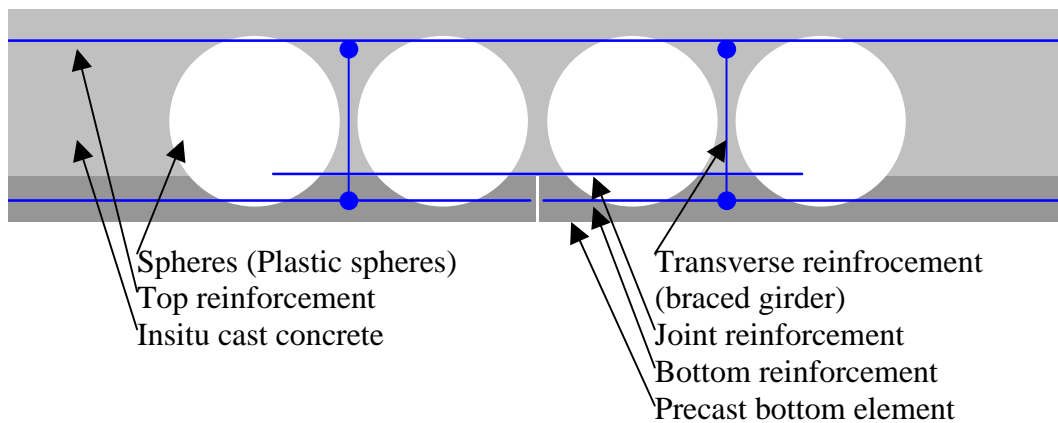
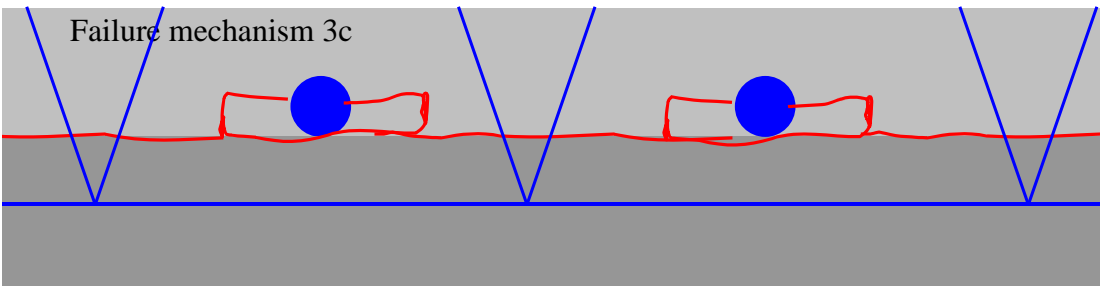
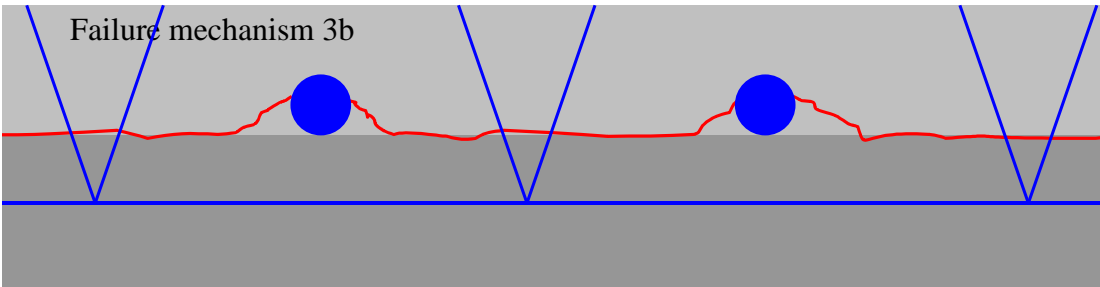
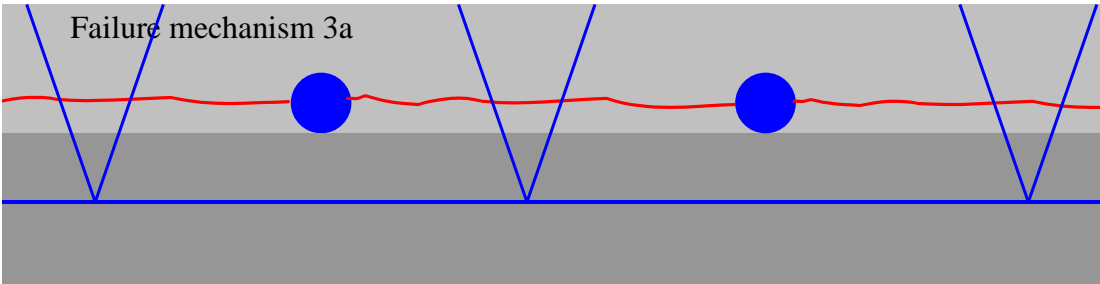
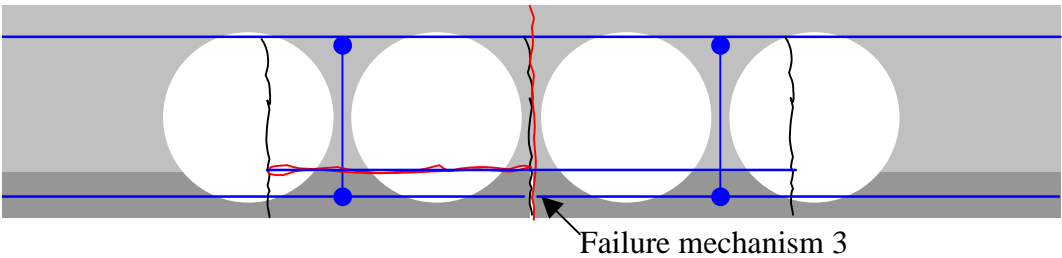
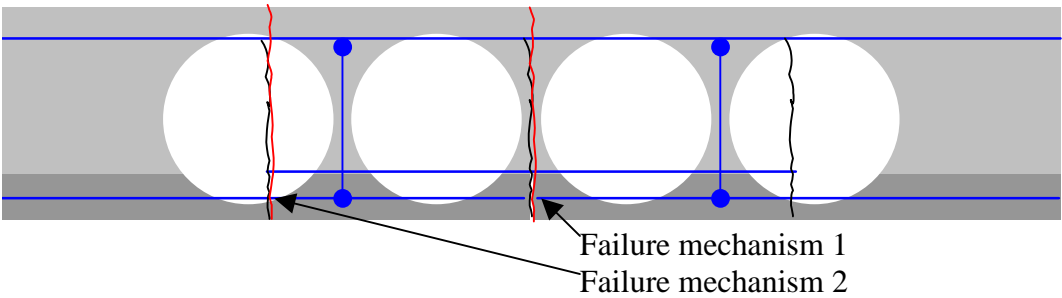


Figure 2.1 Principal sketch of the slab considered.

The moment capacity is determined by studying a number of failure mechanisms. The upper bound approach is used since it is relatively simple to estimate possible failure mechanisms. Furthermore, it is practically impossible to find a lower bound solution to a problem of this sort. However, since an upper bound approach is used and since we have no lower bound solution to the problem we have to make sure that the most important failure mechanisms have been identified.

In the present joint we have the failure mechanisms shown in Figure 2.2.



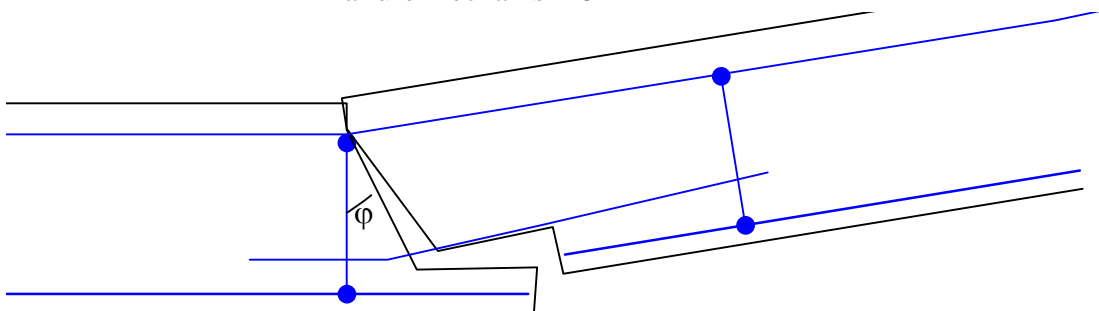
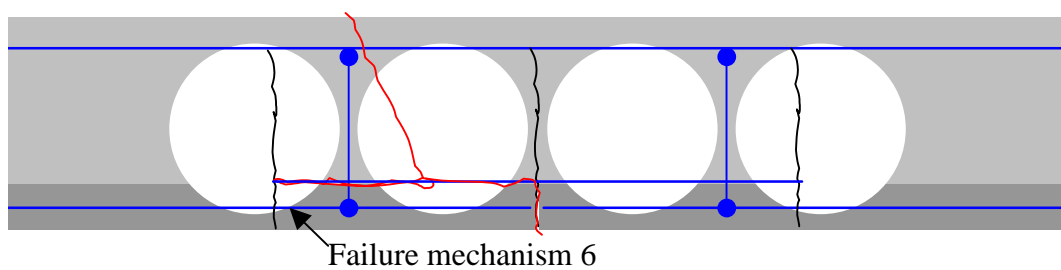
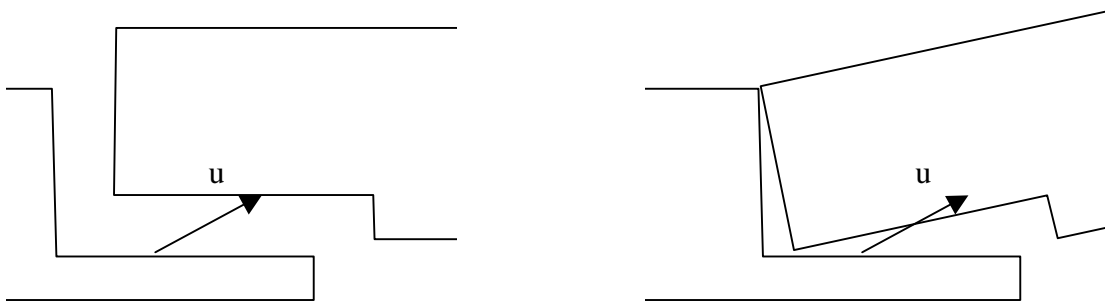
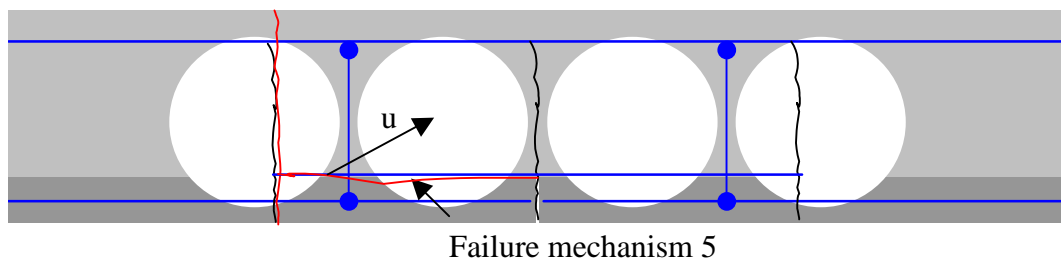
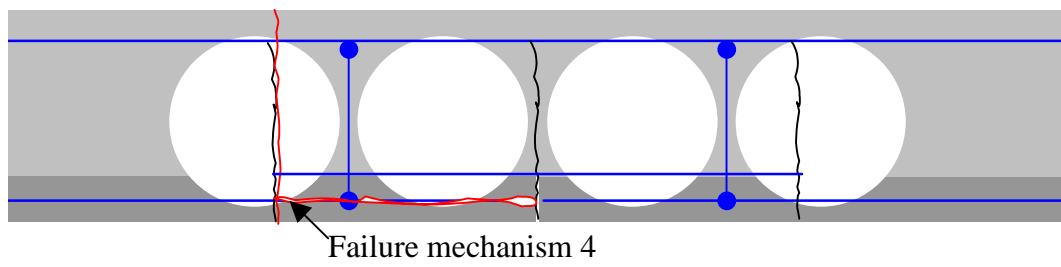


Figure 2.2 Failure mechanisms.

In failure mechanism 1 and 2 we have yielding in the joint reinforcement and the bottom reinforcement. In these cases it is only a matter of determining the bending moment capacity using formula (1.10).

The ductility of this failure is usually very large since yielding in the reinforcement is the decisive factor. Therefore, it is often a desired failure mechanism. This failure mechanism will govern the load carrying capacity if none of failure mechanisms described below occur before yielding of the reinforcement.

Failure mechanism 3a to 3c are different variants of a failure mechanism where the joint reinforcement is pulled out due to the bending of the slab. These mechanisms involve a local failure mechanism and a failure mechanism in the surrounding concrete.

In 3a the failure mechanism in the surrounding concrete is a splitting failure. In this mechanism we have 3 contributions to the dissipation being: local failure, splitting failure and reinforcement contribution.

In 3b the failure mechanism in the surrounding concrete is a combination of a splitting failure and a V-notch failure. In this mechanism we have 4 contributions to the dissipation being: local failure, splitting failure, V-notch failure and reinforcement contribution. However, since the splitting failure in this case takes place in the construction joint the tensile strength should be set to zero here. The tensile strength in a construction joint is in general doubtful. Furthermore in this case tensile stresses in the construction joint occur due to bending as shown in Figure 2.3. It is seen that if the two slab parts would have to follow each other, tension has to be transferred through the construction joint. Since this is not considered possible, the two parts will separate until the separation is terminated by the transverse reinforcement. Therefore, failure mechanism 3b actually only has 3 contributions to the dissipation.

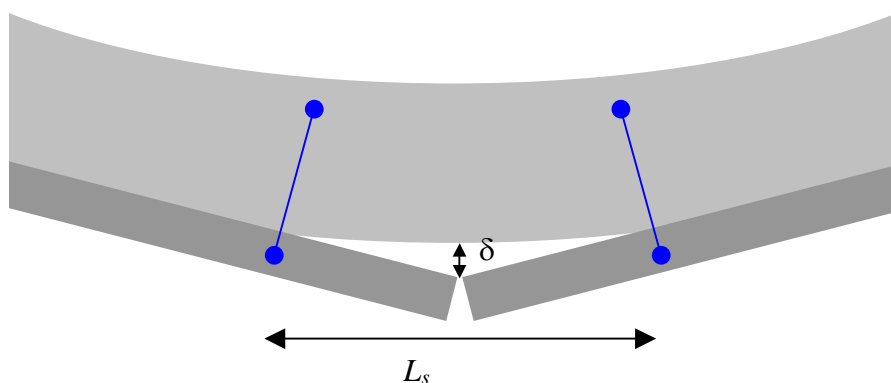


Figure 2.3 Separation due to bending.

In 3c the mechanism in the surrounding concrete is a combination of a splitting failure and a bending failure. In this mechanism we have 4 contributions to the dissipation being: local failure, splitting failure, bending failure and reinforcement contribution. As before the contribution from the splitting failure is set to zero.

Failure mechanism 4 is basically the same as failure mechanism 3 but here the bottom reinforcement is pulled out. Besides the contribution from the local failure, we have a contribution from either V-notch failure, cover bending failure or splitting failure. Whether there is a contribution from the transverse reinforcement or not depends on the position of the transverse reinforcement. Assuming that the transverse reinforcement is placed on top of the longitudinal reinforcement there will be no contribution.

Failure mechanism 5 is a shear failure in the construction joint. Strictly speaking the calculations of a construction joint using the formulas for a rough joint requires that a displacement u , as illustrated in Figure 2.2, is possible and leads to external work. This is not the case since the slab in a failure mechanism as illustrated on the left hand side does not rotate and therefore does not lead to any external work. The failure mechanism on the right hand side is not geometrically possible since the angle between the displacement and the yield line is less than the friction angle. Assuming we have plane strain this is not possible.

A geometrically possible failure mechanism would be a rotation about the line of zero strain of the compression zone combined with a displacement of the bottom slab. Nevertheless it is known that calculating the construction joint as a rough joint is an underestimation of the capacity will be considered here to be a sufficiently good estimate of the capacity of the construction joint.

It is of course required under this assumption that the surface has to be rough. Besides from the requirement to the roughness it is also necessary to evaluate the separation opening δ illustrated in Figure 2.3. If the opening is too large it is not possible to transfer shear stresses along the whole length of the construction joint. The transfer area should only include the area where the opening is not too large.

Finally it is of course necessary to reduce the transfer area due to the presence of the spheres in the BubbleDeck.

Failure mechanism 6 is a pull out of the reinforcement like failure mechanism 3. This failure mechanism is geometrically possible if the slope of the crack in tension is equal

Note on the moment capacity in a Bubble deck joint

to the friction angle. If this requirement is fulfilled, only the pull out of the reinforcement contributes to the internal work. Calculations of this failure mechanism are similar to the calculations of failure mechanism 3. The length of reinforcement that needs to be pulled out is given geometrically as the height of the concrete cast insitu multiplied by $\tan(\text{friction angle})$.

3 A case study, calculation of the actual load carrying capacity

The approach described in this section is the one used if the problem is to determine the actual load carrying capacity. This would be the situation if one wishes to compare the load carrying capacity with experiments. This means that the strengths are inserted as average strengths.

In this case study a slab consisting of a precast bottom slab and a part cast in-situ is considered. The precast part includes a reinforcement net in the bottom of the slab and a so-called SE- grider. The precast part includes a top reinforcement net, plastic spheres (a Bubble deck) and joint reinforcement.

The slab is illustrated in Figure 3.1.

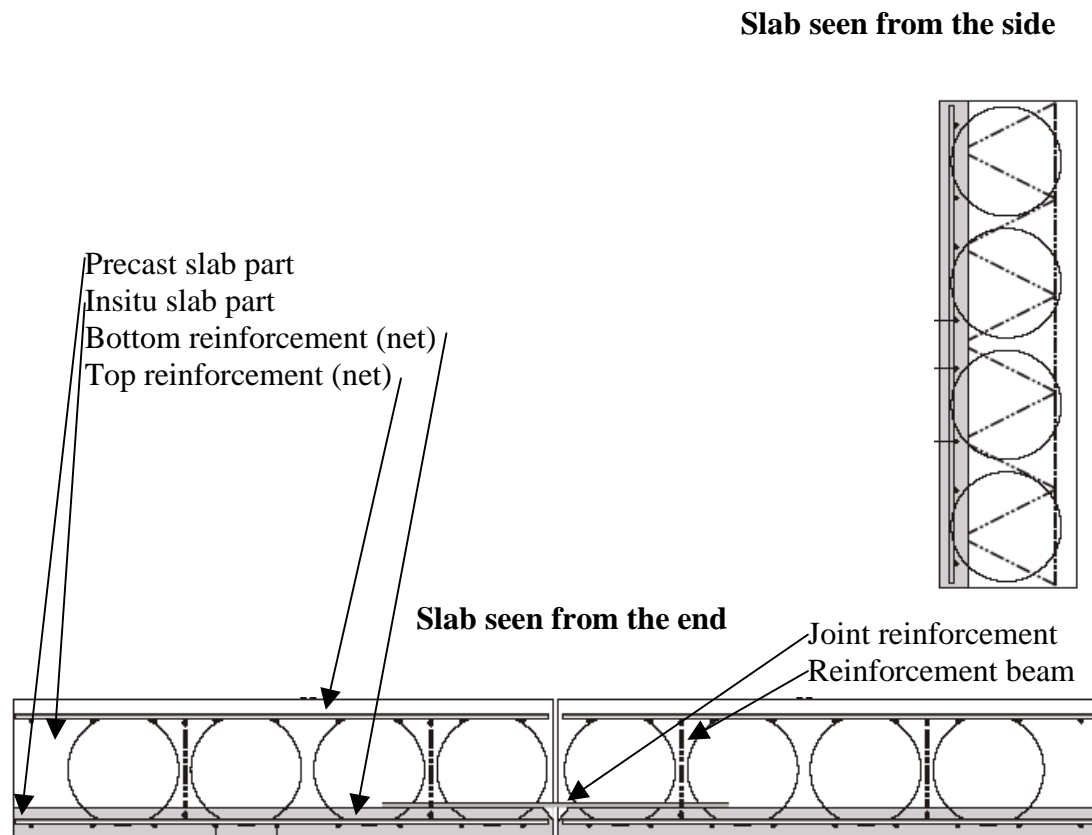


Figure 3.1 Slab used in the case study.

The following data are valid for the slab:

Note on the moment capacity in a Bubble deck joint

Precast concrete as well as in-situ concrete:

$$f_c = 33 \text{ MPa}$$

The bottom slab has a thickness of 60mm and the total depth of the slab is 280mm. The roughness of the slab is 3mm (meaning 3mm high peaks).

The bottom reinforcement is Y8/125 in both directions and the joint reinforcement is Y8/125 as well. The total length of the joint reinforcement is 700mm, 350mm at each side. The yield strength is.

$$f_y = 550 \text{ MPa}$$

The rib depth of the reinforcement is 0.52mm, the width of the ribs is 1.26mm and the center-to-center distance is 5.6mm.

The transverse reinforcement is a SE –girder with $\phi 9$ as diagonals. The depth of the girder is 200mm and the distance between each junction is 200mm.

$$f_{yw} = 500 \text{ MPa}$$

Considering failure mechanism 1 and 2 it is seen that failure mode 1 will be the critical one since the reinforcement is the same but failure mode 1 has less effective depth.

The force per meter corresponding to yielding of the reinforcement is 221kN/m.

In Figure 3.4 the contribution to the dissipation from the different failure mechanisms 3 is shown as a function of the angle α . In these calculations the angle β should be determined as to minimize the dissipation. In this case $\beta = \pi/2 - \phi$. Furthermore $c = 0$ and

$$u_B = 2 \sin(\alpha) \cos\left(A \arctan\left(\frac{100}{200}\right)\right).$$

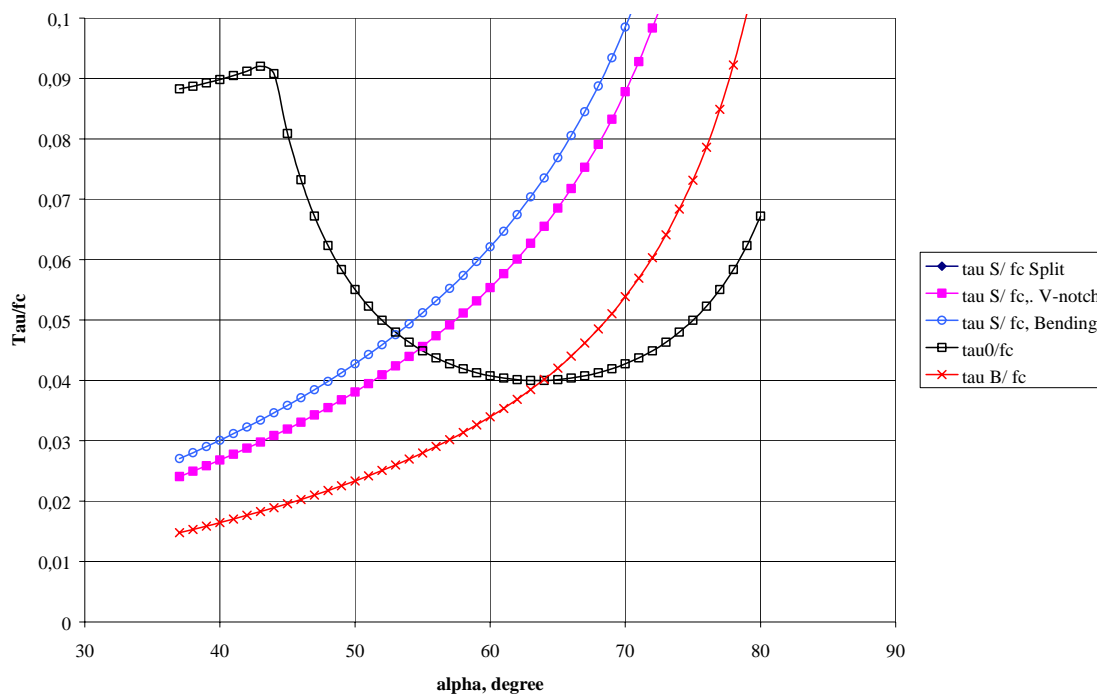


Figure 3.2

It appears that V-notch failure leads to the lower load-carrying capacity. The load corresponding to this failure mechanism is shown in Figure 3.3.

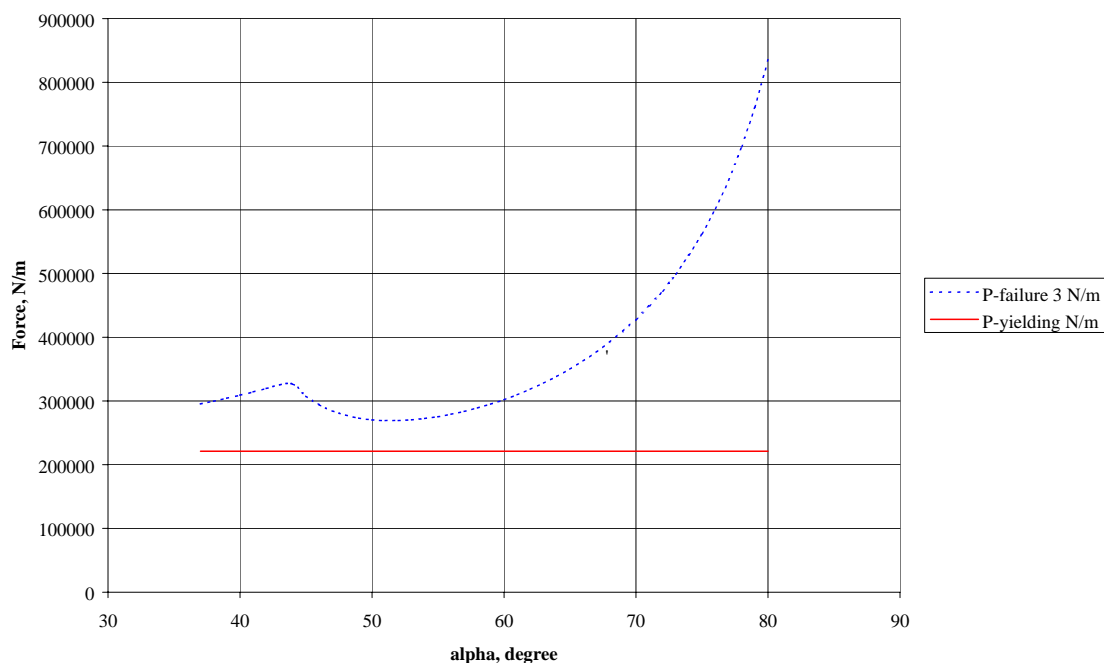


Figure 3.3 Load carrying capacity for failure mechanism 3

Thus failure mechanism 3 requires higher load than the load corresponding to yielding of the reinforcement. The joint reinforcement therefore yields before failure mechanism 3 occurs.

In this case study it is obvious that failure mechanism 4 leads to a higher load carrying capacity than failure mechanism 3 due to the fact that the concrete cover in the bottom slab is larger. Therefore it is unnecessary to investigate this mechanism further.

The separation along the joint may be evaluated by assuming that the top part of the slab has a constant curvature corresponding to yielding of the reinforcement and a compressive strain in the top concrete of 0,35%. Furthermore, it is assumed that the bottom part follows the top part until the transverse reinforcement is reached and that the bottom part has no curvature after this point. This means that the maximum separation may be calculated as:

$$\delta = \frac{1}{8} \kappa L_s^2 = \frac{1}{8} \frac{2.75\text{‰} + 3.5\text{‰}}{220 - 4} 500^2 = 0.9\text{mm} \quad (3.1)$$

L is set to 500mm, which is the distance between the two, the SE-girders. Therefore, it seems reasonable to include the whole area in the calculations of failure mechanism 5. However, a reduction of 60% due to the spheres is of course necessary. Including this in the calculations gives a load carrying capacity of 213kN/m for this failure mechanism.

In failure mechanism 6 it is necessary to determine the distance from the rotation point to the reinforcement in order to calculate the length of reinforcement that needs to be pulled out. The rotation point is at the bottom of the compression zone and in this case it is assumed that the depth of the compression zone may be determined by assuming the reinforcement to be yielding. A concrete strength of 33MPa leads to an effectiveness factor of 0.74 and a depth of the compressive zone of 9mm. The diameter of the reinforcement is 8mm and the roughness is 3mm. Since the angle of friction is 37 degrees, the total length of the reinforcement that needs to be pulled out becomes:

$$l = \tan(37)(220 - 3 - 9 - 8) + (350 - 250) = 251\text{mm} \quad (3.2)$$

The contribution to the dissipation and the force needed to pull out the reinforcement in failure mechanism 6 is shown in Figure 3.4 and Figure 3.5

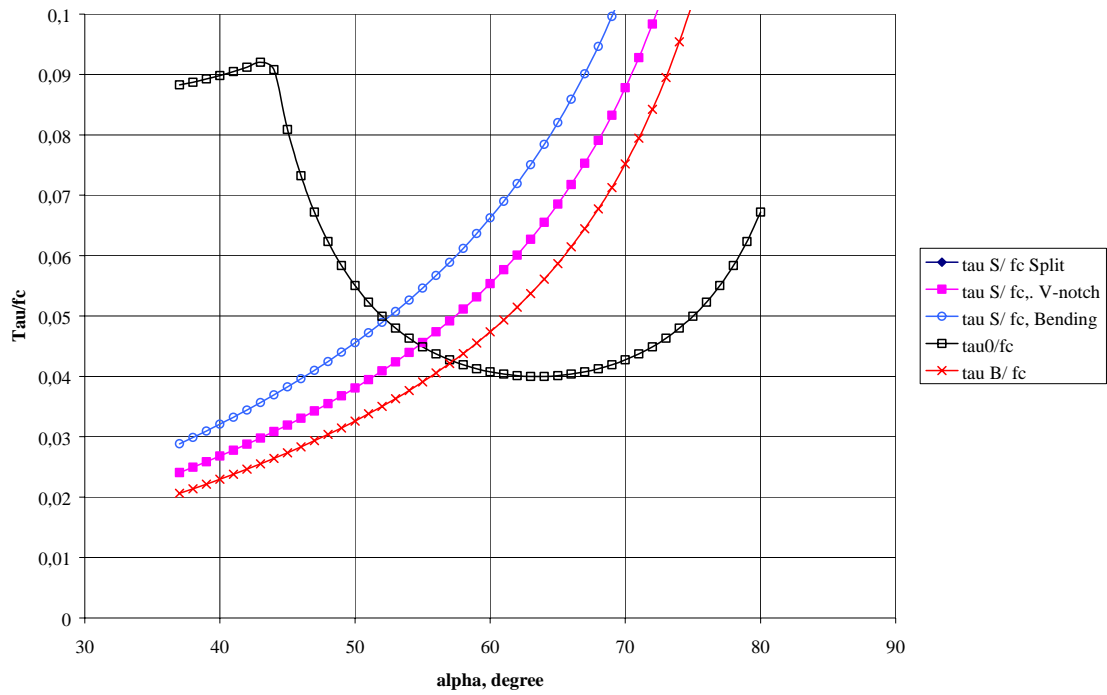


Figure 3.4

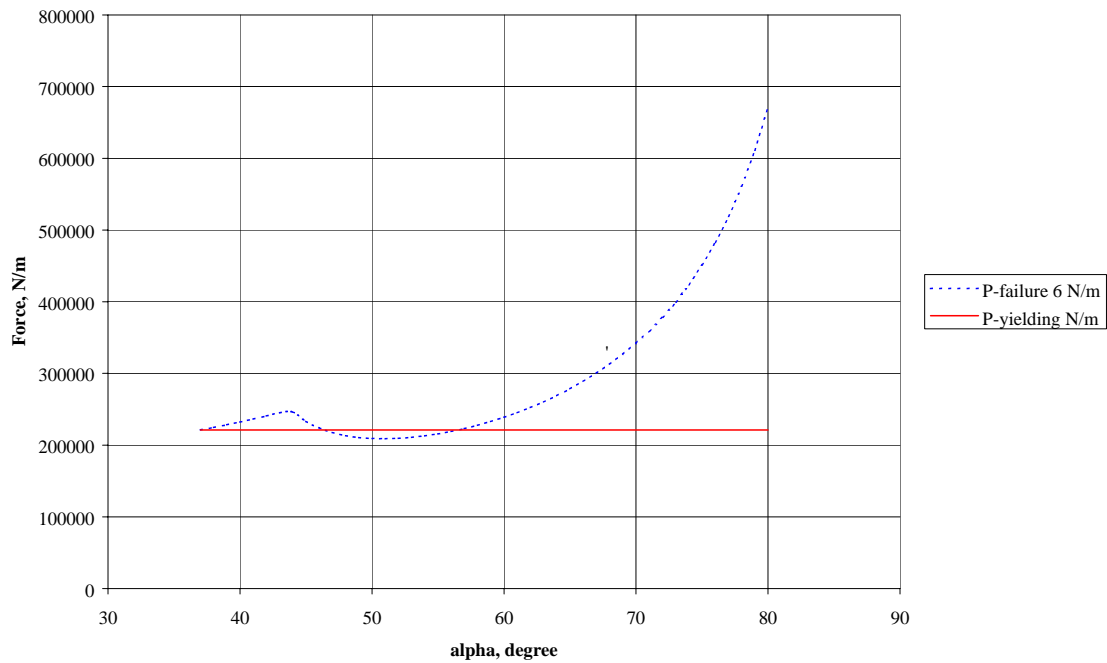


Figure 3.5 Force needed to pull out the reinforcement in failure mechanism 6

Since the force needed in order to pull out the reinforcement (209kN/m) is less than that leading to yielding of the reinforcement, failure mechanism 6 is the most critical one. In the calculation above it is assumed that the depth of the compression zone is 9mm corresponding to yielding of the reinforcement. Calculation of the depth based on the anchorage force leads to a depth of 8.6mm and no recalculation is needed.

Note on the moment capacity in a Bubble deck joint

The moment capacity may now be determined from (1.10) where the anchorage force replaces the yield strength multiplied with the reinforcement area. The effective depth, d , is set to $220-3-4=213\text{mm}$. This leads to a value of 43.6 kNm/m .

4 A case study, the design situation

The approach described in this section is the one used for determination of the design load carrying capacity. The section illustrates how to safety factors when calculating design strengths and the design load carrying capacity.

We shall assume normal safety class and normal control class according to the Danish Code DS411, 1999.

In this case study a slab consisting of a precast bottom slab and a part cast in-situ is considered. The precast part includes a reinforcement net in the bottom of the slab and a so-called SE- grider. The precast part includes a top reinforcement net, plastic spheres (a Bubble deck) and joint reinforcement.

The slab is illustrated in Figure 4.1.

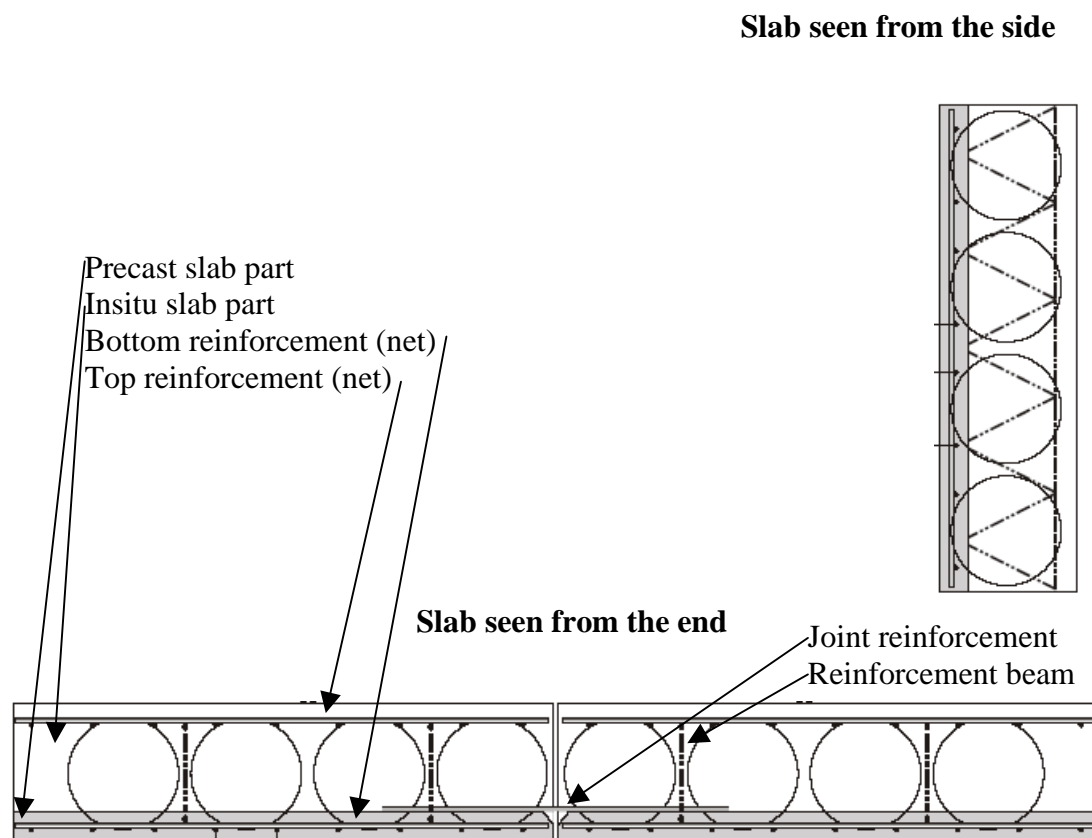


Figure 4.1 Slab used in the case study.

The following data are valid for the slab:

Precast concrete as well as in-situ concrete:

Note on the moment capacity in a Bubble deck joint

$$f_{ck}= 35\text{MPa}$$

$$f_{cd}= 21\text{MPa} \quad (\text{Safety factor } \gamma_c=1.65)$$

The bottom slab has a thickness of 60mm and the total depth of the slab is 280mm. The roughness of the slab is 3mm (meaning 3mm high peaks).

The bottom reinforcement is Y8/125 in both directions and the joint reinforcement is Y8/125 as well. The total length of the joint reinforcement is 700mm, 350mm at each side. The yield strength is:

$$f_{yk}= 550\text{MPa}$$

$$f_{yd}= 423\text{MPa} \quad (\text{Safety factor } \gamma_s=1.3)$$

The rib depth of the reinforcement is 0.52mm, the width of the ribs is 1.26mm and the center-to-center distance is 5.6mm.

The transverse reinforcement is a SE –girder with $\varnothing 9$ diagonals. The depth of the girder is 200mm and the distance between each junction is 200mm.

$$f_{ywk}= 500\text{MPa}$$

$$f_{ywd}= 385\text{MPa}$$

Considering failure mechanism 1 and 2 it is seen that failure mode 1 will be the critical one since the reinforcement is the same but failure mode 1 has less effective depth.

The force per meter corresponding to yielding in the reinforcement is 170kN/m.

In Figure 4.2 the contribution to the dissipation from the different failure mechanisms 3 is shown as a function of the angle α . In these calculations the angle β should be determined as to minimize the dissipation. In this case $\beta = \pi/2 - \varphi$. Furthermore $c = 0$ and

$$u_B = 2 \sin(\alpha) \cos\left(\arctan\left(\frac{100}{200}\right)\right).$$

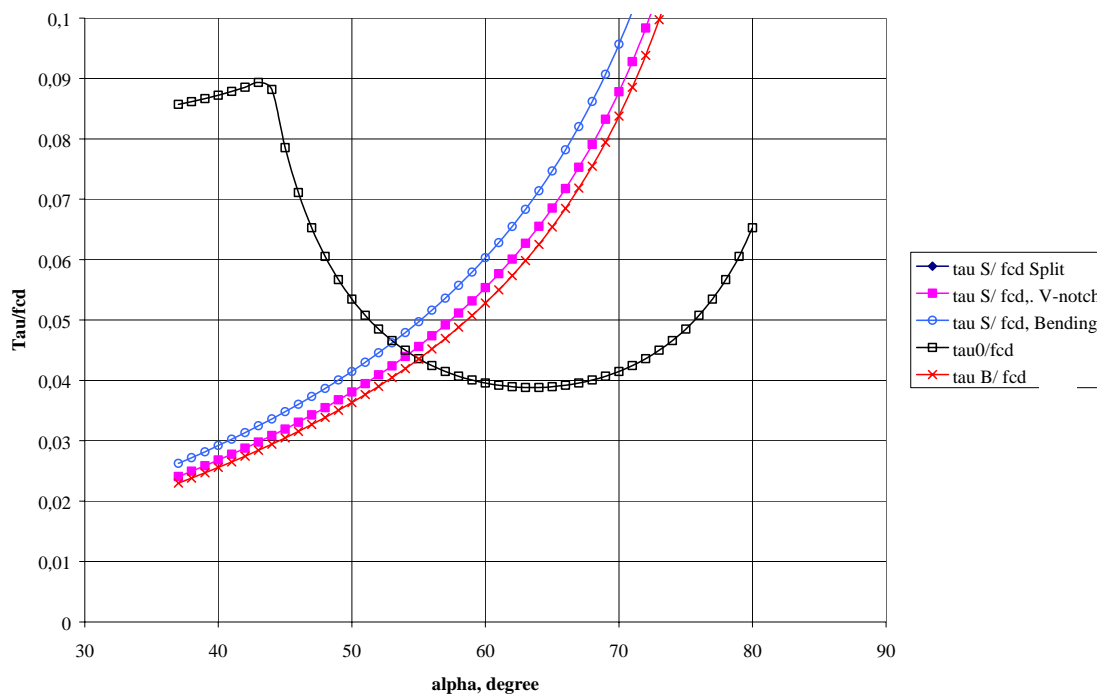


Figure 4.2

It appears that V-notch failure leads to the lower load-carrying capacity. The load corresponding to this failure mechanism is shown in Figure 4.3

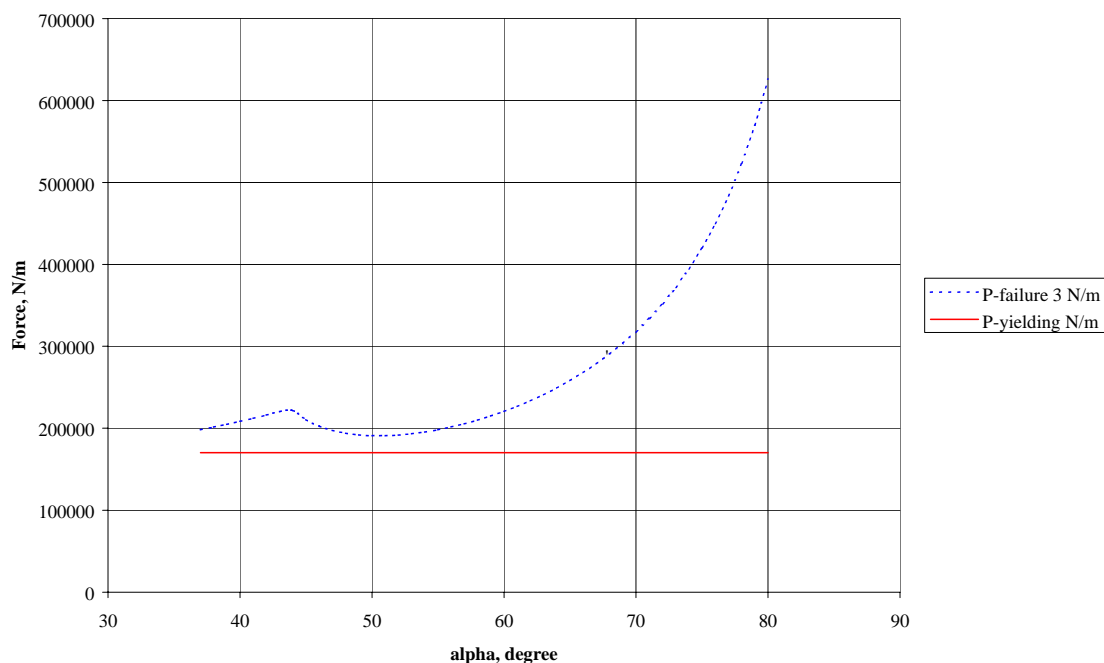


Figure 4.3 Load carrying capacity for failure mechanism 3

Thus failure mechanism 3 requires higher load than the load corresponding to yielding of the reinforcement. The joint reinforcement therefore yields before failure mechanism 3 occurs.

In this case study it is obvious that failure mechanism 4 leads to a larger load carrying capacity than failure mechanism 3 due to the fact that the concrete cover in the bottom slab is larger. Therefore it is unnecessary to investigate this mechanism further.

The separation along the joint may be evaluated by assuming that the top part of the slab has a constant curvature corresponding to yielding of the reinforcement and a compressive strain in the top concrete of 0.35%. Furthermore, it is assumed that the bottom part follows the top part until the transverse reinforcement is reached and that the bottom part has no curvature after this point. This means that the maximum separation may be calculated as:

$$\delta = \frac{1}{8} \kappa L_s^2 = \frac{1}{8} \frac{2.75\text{‰} + 3.5\text{‰}}{220 - 4} 500^2 = 0.9\text{mm} \quad (4.1)$$

Therefore, it seems reasonable to include the whole area in the calculations of failure mechanism 5. However, a reduction of 60% due to the spheres is of course necessary. Including this in the calculations gives a load carrying capacity of 164kN/m for this failure mechanism.

In failure mechanism 6 it is necessary to determine the distance from the rotation point to the reinforcement in order to calculate the length of reinforcement that needs to be pulled out. The rotation point is at the bottom of the compression zone and in this case it is assumed that the depth of the compression zone may be determined assuming the reinforcement to be yielding. A characteristic concrete strength f_{ck} of 35MPa leads to an effectiveness factor of 0.73 and a depth of the compressive zone of 11mm. The diameter of the reinforcement is 8mm and the roughness is 3mm. Since the angle of friction is 37 degrees the total length of the reinforcement that needs to be pulled out becomes:

$$l = \tan(37)(220 - 3 - 11 - 8) + (350 - 250) = 249\text{mm} \quad (4.2)$$

The contribution to the dissipation and the force needed to pull out the reinforcement in failure mechanism 6 is shown in Figure 4.4 and Figure 4.5

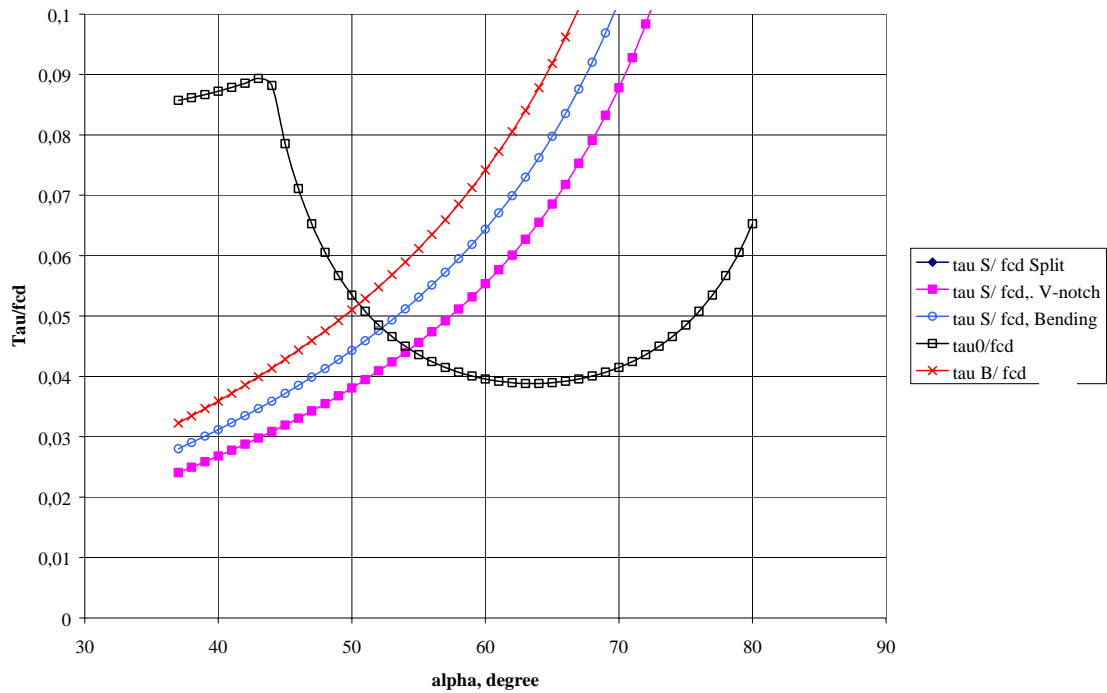


Figure 4.4

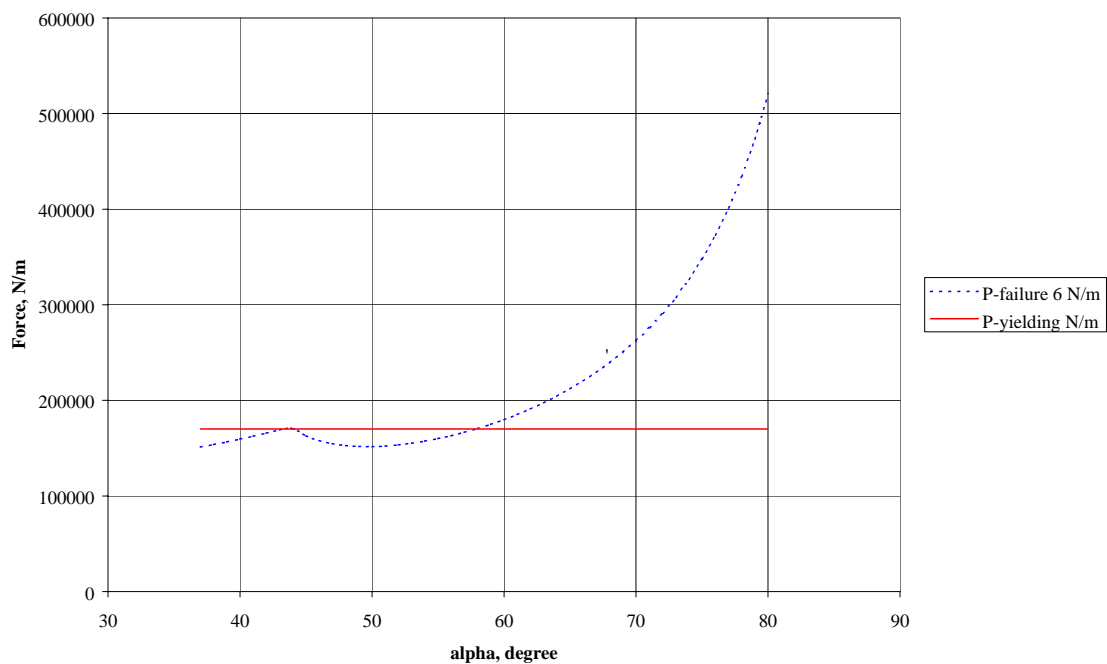


Figure 4.5 Force needed to pull out the reinforcement in failure mechanism 6

Since the force needed in order to pull out the reinforcement (151kN/m) is less than the force corresponding to yielding of the reinforcement, failure mechanism 6 is the most critical one. In the calculation above it is assumed that the height of the compression zone is 11mm corresponding to yielding of the reinforcement. Calculation of the depth based on the anchorage force leads to a depth of 10mm and no recalculation is needed.

Note on the moment capacity in a Bubble deck joint

The moment capacity may now be determined from (1.10) where the anchorage force replaces the yield strength multiplied with the reinforcement area. The effective depth is set to $220 - 3 \cdot 4 = 213 \text{ mm}$. This leads to a value of 31.4 kNm/m .

5 Conclusions

It has been shown in the note how the load carrying capacity of a joint in a Bubble deck may be calculated using the theory of plasticity.

A direct use of code rules is impossible in such a complicated case. Therefore the note also demonstrates the advantage of having a theory in stead of relying on empirical rules with doubtful extrapolations.

6 Literature

- [1] NIELSEN, M. P.: Limit Analysis and Concrete Plasticity, *Second Edition*,
CRC Press, 1998.